

# Elastic response of [111]-tunneling impurities

Peter Nalbach, Orestis Terzidis\*

*Institut für Theoretische Physik, Universität Heidelberg,  
Philosophenweg 19, 69120 Heidelberg, Germany*

Karen A. Topp

*Laboratory of Atomic and Solid State Physics  
Cornell University, Ithaca, New York, 14853*

Alois Würger

*Université Bordeaux 1, CPMOH†,  
351 cours de la Libération, 33405 Talence, France*

November 3, 2018

## Abstract

We study the dynamic response of a [111] quantum impurity, such as lithium or cyanide in alkali halides, with respect to an external field coupling to the elastic quadrupole moment. Because of the particular level structure of a eight-state system on a cubic site, the elastic response function shows a biexponential relaxation feature and a van Vleck type contribution with a resonance frequency that is twice the tunnel frequency  $\Delta/\hbar$ . This basically differs from the dielectric response that does not show relaxation. Moreover, we show that the elastic response of a [111] impurity cannot be reduced to that of a two-level system. In the experimental part, we report on recent sound velocity and internal friction measurements on KCl doped with cyanide at various concentrations. At low doping (45 ppm) we find the dynamics of a single [111] impurity, whereas at higher concentrations (4700 ppm) the elastic response rather indicates strongly correlated defects. Our theoretical model provides a good description of the temperature dependence of  $\delta v/v$  and  $Q^{-1}$  at low doping, in particular the relaxation peaks, the absolute values of the amplitude, and the resonant contributions. From our fits we obtain the value of the elastic deformation potential  $\gamma_t = 0.192$  eV.

## 1 Introduction

The low-temperature properties of alkali halides may be significantly modified by the presence of substitutional impurities, such as Li, CN, or OH. Already a few ppm of these defects

---

\*currently at SAP Labs France, 505 route des Lucioles, F-06560 Valbonne

†Unité Mixte de Recherche CNRS 5798

totally change the thermal behavior and the elastic and dielectric response below Helium temperature.

Regarding the polar molecules CN and OH, the point symmetry of the impurity site gives rise to several equivalent orientations; corresponding off-center positions arise for the small lithium ion. Quantum tunneling between these states results in a ground state splitting of about 1 Kelvin. Since the number of such tunneling states exceeds, even at low concentration, the number of small-frequency phonon modes of the host crystal, the impurities govern the low-temperature properties of the material. The cubic symmetry of fcc crystals favors 8 defect positions in  $[111]$ -directions (CN and Li) or 6 positions in  $[100]$ -directions (OH in KCl). The resulting energy spectra have been discussed in detail by Gomez et al [1], and agree well with the Schottky peak observed by Pohl and co-workers for various impurity systems at low doping [2].

In this paper we are concerned with the elastic susceptibility of a  $[111]$ -impurity. Because of the cubic symmetry, such a tunneling system behaves in many respects as an ensemble of three two-level systems with energy splitting  $\Delta$  [2, 3]. For example, the specific heat contribution of a  $[111]$ -impurity is three times the Schottky peak of a two-state system. A similar relation holds true for the dielectric response function, since the dipolar transitions occur between adjacent levels only, as indicated by the dashed lines in the actual energy spectrum shown in Fig. 1. This analogy has been used to describe lithium or cyanide defects in terms of a two-state approximation [4, 5, 6, 7, 8].

The elastic response function, however, shows a more complex behavior, resulting from the tensor character of the quadrupole operator  $Q_{ij}$  and the structure of the energy spectrum shown in Fig. 1. According to the allowed quadrupolar transitions indicated by solid arrows in Fig. 1, sound waves or external stress perturb the impurity in two ways: First, they mix states separated by twice the splitting, giving rise to a van Vleck type susceptibility with resonance frequency  $2\Delta/\hbar$ . Second, they lift the degeneracy of the states of a given triplet level, resulting in a relaxation contribution to the response function.

Early measurements in KCl:CN samples [9] in the classical regime ( $k_B T \gg \Delta$ ) showed that the change of sound velocity of a  $T_{2g}$ -mode ( $\hat{\mathbf{e}} = [110]$ ,  $\hat{\mathbf{k}} = [001]$ ) varies as expected like  $1/T$  with temperature. Yet in addition, these experiments showed a change of sound velocity for an  $E_g$ -mode ( $\hat{\mathbf{e}} = [110]$ ,  $\hat{\mathbf{k}} = [1-10]$ ) with an amplitude of about ten times smaller than the  $T_{2g}$  ones, whereas this mode should be unaffected according to the simplest model of a symmetric  $[111]$ -tunneling defect.

When measuring the sound velocity (  $T_{2g}$ -mode ) of KCl:Li as a function of temperature in the tunneling regime, Hübner et al. found a hump at  $k_B T \approx \Delta$  [10]. They related this observation to relaxational transitions between degenerate states, by calculating the static elastic response as the second derivative of the free energy of the impurity ion. Their results are valid in the low-frequency limit, where the external frequency is smaller than the impurity relaxation rates.

The internal friction, however, cannot be obtained from a static theory, and the low-frequency limit is not always justified for the sound velocity. Starting from standard dynamic perturbation theory, we develop a dynamic theory for the elastic response function of a  $[111]$ -impurity coupled to a phonon heat bath. The main purpose of this paper is to point out the peculiarities of the elastic response function that arise from the degenerate states of the energy

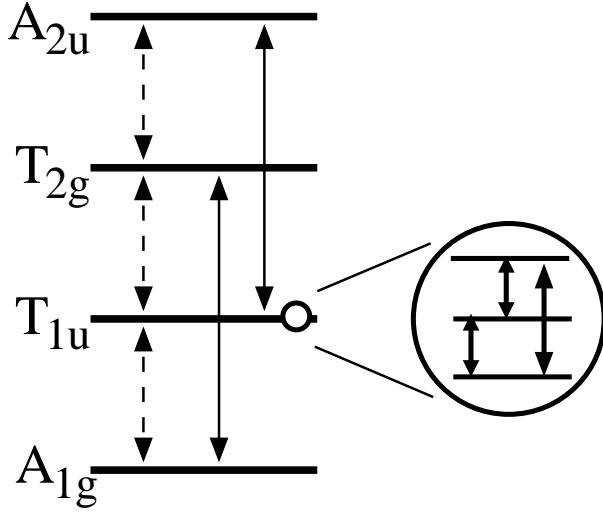


Figure 1: Energy spectrum of a [111]-impurity with zero asymmetry energy. Dashed arrows indicate the allowed dipolar transitions, and full arrows the quadrupolar ones.

spectrum shown in Fig. 1. Moreover, we report sound velocity and internal friction data of a  $T_{2g}$ -mode for KCl doped with cyanide molecules, and discuss them in terms of our [111]-impurity model with damping.

The outline of our paper is as follows. In Sec. II we present the model and the basic equations for the elastic response function of a single impurity. The temperature dependence of the internal friction and sound velocity is evaluated in Sec. III. In Sec. IV we give some details of the experiments on KCl:CN, which are discussed in Sec. V. The final section contains a summary.

## 2 Theory

### 2.1 Quantum operators of a [111]-impurity

We start by discussing the properties of the energy eigenstates and by presenting our notation based on pseudospin operators. As shown in Fig. 1, the energy spectrum contains four equidistant levels; the upper and lower ones,  $A_{1g}$  and  $A_{2u}$ , are single quantum states, whereas the middle levels  $T_{1u}$  and  $T_{2g}$  are threefold degenerate. This groundstate multiplet can be described as the direct product of three two-level systems with energy splitting  $\Delta$ .

Each energy eigenstate is a superposition of states  $|\mathbf{r}\rangle$  localized at the eight impurity positions

$$\mathbf{r} = \frac{1}{2}d(\sigma_z^1, \sigma_z^2, \sigma_z^3) \quad (1)$$

with the effective two-state coordinates  $\sigma_z^i$ . For a lithium impurity, the off-center positions  $\mathbf{r}$  form a cube of side-length  $d$ , whereas for cyanide impurities  $\mathbf{r}$  indicates the orientation of the cigar-shaped polar molecule. Due to quantum tunneling along the axes  $i = 1, 2, 3$ , the

energy eigenstates factorize as  $|\sigma_x^1\rangle|\sigma_x^2\rangle|\sigma_x^3\rangle$ , where the variables  $\sigma_x^i = \pm 1$  label odd and even superpositions  $|\sigma_x^i\rangle = 2^{-1/2} \{ |r_i = d/2\rangle + \sigma_x^i |r_i = -d/2\rangle \}$  along the  $i$ -axis.

Accordingly, the quantum operators of the impurity may be written as direct products of pseudospin operators  $\sigma_\alpha^i$ , where  $\alpha = x, y, z$  label the usual Pauli matrices and  $\alpha = 0$  the identity operator. In terms of quantum states at  $r_i = \pm d/2$  we have

$$\sigma_x^i = |d/2\rangle\langle -d/2| + | -d/2\rangle\langle d/2| \quad (2)$$

$$\sigma_z^i = |d/2\rangle\langle d/2| - | -d/2\rangle\langle -d/2| \quad (3)$$

Thus a lithium or cyanide impurity is described as the product of three two-state variables. We adopt the shorthand notation for its quantum operators

$$A_{\alpha\beta\gamma} = \sigma_\alpha^1 \otimes \sigma_\beta^2 \otimes \sigma_\gamma^3, \quad (4)$$

where  $i = 1, 2, 3$  label the crystal axes and Greek indices  $\alpha = 0, x, y, z$  the pseudospin operators. When denoting by  $\frac{1}{2}\Delta$  the tunneling amplitude between adjacent impurity positions, we obtain the Hamiltonian

$$H_S = -\frac{\Delta}{2} (A_{x00} + A_{0x0} + A_{00x}). \quad (5)$$

Its eigenstates may be labelled according to the eigenvalues  $\pm 1$  of  $\sigma_x^i$ ; for example, the ground state  $A_{1g}$  reads as  $|+++ \rangle$ , and the states of the triplet level  $T_{1u}$  as  $| -++ \rangle$ ,  $| +-+ \rangle$ , and  $| ++- \rangle$ . According to the above discussion, the statistical operator  $\rho = e^{-\beta H_S} / \text{tr}(e^{-\beta H_S})$  factorizes as

$$\rho = \rho^1 \otimes \rho^2 \otimes \rho^3, \quad \rho^i = \frac{1}{2} \left( 1 + \sigma_x^i \tanh(\Delta/2k_B T) \right). \quad (6)$$

(In the limit of zero temperature, the even state  $\sigma_x^i = 1$  is occupied with probability 1.) From the statistical operator it is evident that the specific heat anomaly due to  $N$  such defects is identical to the Schottky peak of  $3N$  two-level systems with the Hamiltonian  $\frac{1}{2}\Delta\sigma_x$ . As to the dynamic properties, a similar relation holds true for the dielectric susceptibility. This is not surprising, since dipolar transitions involve a single coordinate  $r_i$  and occur between adjacent levels with splitting  $\Delta$  only; cf. Fig. 1.

A different situation, however, is encountered when considering the elastic response: The quadrupole operator

$$Q_{ij} = r_i r_j (1 - \delta_{ij}) \quad (7)$$

involves two coordinates, and hence causes transitions between energy eigenstates that differ in two labels  $\sigma_x^i$ . Thus elastic perturbations induce two types of transitions as indicated by the solid arrows in Fig. 1.

## 2.2 Phonon coupling

Noting (1) and  $A_{z00}A_{0z0} = A_{zz0}$ , we may write the quadrupole operators as  $Q_{12} = (d/2)^2 A_{zz0}$ , etc. When absorbing the factor  $(d/2)^2$  in the coupling constant  $\gamma$ , we obtain the impurity-phonon interaction [8]

$$H_{SB} = 2 \sum_{\alpha} \gamma_{\alpha} (A_{zz0} \epsilon_{12}^{\alpha} + A_{z0z} \epsilon_{13}^{\alpha} + A_{0zz} \epsilon_{23}^{\alpha}). \quad (8)$$

When evaluating the strain tensor at the impurity site  $\mathbf{R}$  and taking the limit of long wavelengths,  $kd \ll 1$ , we find

$$\epsilon_{ij}^\alpha = \frac{i}{2} \sum_{\mathbf{k}} \sqrt{\frac{\hbar}{2m\omega_{\mathbf{k}\alpha}}} e^{i\mathbf{k}\mathbf{R}} \left( e_i^\alpha(\mathbf{k})k_j + e_j^\alpha(\mathbf{k})k_i \right) \left( b_{\mathbf{k},\alpha} + b_{-\mathbf{k},\alpha}^\dagger \right). \quad (9)$$

Here  $\mathbf{k}$  and  $\mathbf{e}^\alpha$  are wave and polarisation vectors, and  $\alpha$  labels the longitudinal and transverse phonon branches.

### 2.3 Asymmetry energy

Up to now we have considered an impurity in a potential that reflects the cubic site symmetry. The strong dipolar and elastic interactions of nearby impurities, however, break that symmetry and give rise to an effective asymmetry energy,

$$V = -\frac{v_1}{2} A_{z00} - \frac{v_2}{2} A_{0z0} - \frac{v_3}{2} A_{00z}, \quad (10)$$

where the  $v_i$  are random quantities with zero mean. We assume a Gaussian distribution with width  $\sigma$ :

$$P(\vec{v}) = \prod_i P_i(v_i) \quad \text{with} \quad P_i(v_i) = \frac{1}{\sqrt{2\pi}\sigma} \exp\left(-\frac{1}{2} \frac{v_i^2}{\sigma^2}\right) \quad (11)$$

In principle, the  $v_i$  are dynamic variables closely related to the position operators of nearby impurities. In the case of weak interaction,  $v_i \ll \Delta$ , however, they may be treated as static random fields. Eq. (10) accounts for random fields arising from dipolar interactions; elastic coupling would lead to a potential that involves quadrupole operators such as  $A_{zz0}$ .

## 3 Elastic response function

The lattice vibrations of the host crystal act on the tunneling impurity as a heat bath at temperature  $T$ . Upon a perturbation by an external strain field, the impurity regains the thermal equilibrium through absorption or emission of resonant phonons. Since the impurity-phonon coupling is weak, the resulting damping rates can be evaluated in second-order perturbation theory.

### 3.1 Dynamic perturbation theory

The linear response of the impurity to a time-dependent external strain field is described by the commutator correlation function  $\langle [Q_{ij}(t), Q_{ij}] \rangle$ . For convenience, we use dimensionless quadrupole operators, e.g.  $A_{zz0} = (2/d)Q_{12}$  with  $\langle A_{zz0}^2 \rangle = 1$ ; all relevant response functions can be expressed in terms of

$$\chi(t) = \langle [A_{zz0}(t), A_{zz0}] \rangle \quad (12)$$

It turns out convenient to calculate first the correlation matrix

$$C_{\alpha\beta\gamma;\delta\epsilon\zeta}(t) = \langle A_{\alpha\beta\gamma}(t) | A_{\delta\epsilon\zeta} \rangle, \quad (13)$$

where we have defined the symmetrized correlation function

$$(A|B) = \frac{1}{2}\langle AB + BA \rangle. \quad (14)$$

Our evaluation of the correlation matrix is based on the Mori-Zwanzig projection formalism; the resulting memory kernel is calculated to second order in the impurity-phonon coupling [11]. Thus we obtain a matrix equation for the Laplace transform of (13),

$$C(z) = \frac{-1}{z - \Omega - K(z)} M, \quad (15)$$

with the usual definitions of the static correlations

$$M_{mn} = (A_m|A_n) = (\eta^{-1})_{mn}, \quad (16)$$

the frequency matrix

$$\Omega_{mn} = (A_m|\mathcal{L}A_p)\eta_{pn}, \quad (17)$$

and the memory kernel

$$K_{mn}(z) = (\dot{A}_m|(z - \mathcal{L}_0)^{-1}|\dot{A}_p)\eta_{pn}. \quad (18)$$

For convenience, we have replaced the triple index pair of (4) with  $m, n$ , and we have used the shorthand notations  $\dot{A}_i = i[H_{SB}, A_i]$  and  $\hbar\mathcal{L}_0* = [H_S + H_B, *]$ , where  $H_B = \sum \hbar\omega_k b_k^\dagger b_k$ . The thermal average  $\langle \dots \rangle$  is with respect to  $\rho$  and the equilibrium distribution of the phonons.

Solving the impurity dynamics now amounts to calculating the eigenvalues und residues of the resolvent  $[z - \Omega - K]^{-1}$ . Since there are  $4^3$  operators  $A_{\alpha\beta\gamma}$ , the matrix equation involves a 64-dimensional space. The matrices  $C$ ,  $M$ ,  $\Omega$ , and  $K$  being block-diagonal, the actual problem simplifies significantly.

For symmetry reasons, the time evolution of the three operators  $A_{zz0}$ ,  $A_{z0z}$ , and  $A_{0zz}$  is the same. Therefore it is sufficient to evaluate the dynamics in the invariant subspace containing one of them, e.g.,

$$\begin{aligned} A_1 &= A_{zz0}, \quad A_2 = A_{zy0}, \quad A_3 = A_{yz0}, \quad A_4 = A_{yy0}, \\ A_5 &= A_{zzx}, \quad A_6 = A_{zyx}, \quad A_7 = A_{yzx}, \quad A_8 = A_{yyx}. \end{aligned} \quad (19)$$

In this invariant subspace,  $\Omega$ ,  $M$ , and  $K$  are represented by  $8 \times 8$ -matrices that are easily calculated according to (16–18). Note that the commutation relations for the operators  $A_i$  can be traced back to those for Pauli matrices. It can be shown that  $\Omega$  and  $M$  can be diagonalized simultaneously; in the present example it is straightforward to find the corresponding unitary transformation  $U$  and to obtain

$$\tilde{\Omega} = U^\dagger \Omega U = \text{diag}(0, 0, 0, 0, -2\Delta, -2\Delta, 2\Delta, 2\Delta)/\hbar \quad (20)$$

$$\tilde{M} = U^\dagger M U = \text{diag}(m_1, m_1, m_2, m_2, m_3, m_4, m_3, m_4) \quad (21)$$

with

$$\begin{aligned} m_1 &= (1 - t)(1 - t^2) \\ m_2 &= (1 + t)(1 - t^2) \\ m_3 &= (1 + t)(1 + t^2) \\ m_4 &= (1 - t)(1 + t^2) \end{aligned}$$

where we have used  $\beta = 1/k_B T$  and  $t = \tanh(\beta\Delta/2)$ .

Besides the fourfold degenerate zero frequency, there are two doubly degenerate finite frequencies  $\pm 2\Delta/\hbar$  in Liouville space. While  $\Omega$  and  $M$  could be diagonalized simultaneously, this is not possible for the memory matrix  $K$ . It turns out, however, that its transform  $\tilde{K}$  is diagonal in each of the three degenerate subspaces of  $\tilde{\Omega}$ , with bare frequencies  $0, \pm 2\Delta/\hbar$ ; the finite off-diagonal entries connect, e.g., the subspace of zero frequency eigenvalue with that of eigenvalue  $2\Delta/\hbar$ . Because of  $\tilde{K} \ll \Delta/\hbar$ , we may neglect these off-diagonal entries of  $\tilde{K}$ ; they would result in very small corrections to the frequencies and residues of the order of  $(\hbar\tilde{K}/\Delta)^2$ . In physical terms, the off-diagonal parts of  $\tilde{K}$  in the degenerate subspaces vanish, since they involve the phonon density of states at zero frequency; in a three-dimensional body, however, the density of phonon modes vanishes in the limit  $\omega_k \rightarrow 0$ .

Applying the usual Markov approximation, we evaluate the memory functions  $\tilde{K}(z)$  at the corresponding bare frequencies  $z = 0, \pm 2\Delta/\hbar$ . It turns out convenient to separate real and imaginary parts according to  $\tilde{K} = \tilde{K}' + i\tilde{K}''$ . Whereas the entries in the subspace of zero eigenvalue are purely imaginary, those belonging to the finite frequencies  $\pm 2\Delta/\hbar$  are complex numbers. Their real parts  $\tilde{K}'(\pm 2\Delta/\hbar)$  would induce a shift of the resonance frequencies from the bare values  $\pm 2\Delta/\hbar$  to slightly smaller ones. This shift being very small, we discard it and retain the imaginary, or dissipative, part  $\tilde{K}''$  only. The latter form a diagonal matrix  $\tilde{\Gamma} = \Im \tilde{K}''(z_0)$  with  $z_0 = 0, \pm 2\Delta/\hbar$ .

With these approximations for the memory kernel,  $\tilde{\Omega}$ ,  $\tilde{M}$ , and  $\tilde{\Gamma}$  are diagonal; the correlation matrix thus factorizes,

$$\tilde{C}_{jj}(z) = \frac{-\tilde{M}_{jj}}{z - \tilde{\Omega}_{jj} + i\tilde{\Gamma}_{jj}}, \quad (22)$$

where  $j = 1, \dots, 8$  labels the eight eigenvalues given in (20,21) and those of the damping matrix  $\tilde{\Gamma}$ . Since we are interested in the correlation function of the operator  $A_{zz0}$ , we have to calculate the element  $C_{11}$  of the correlation matrix in the original basis,  $C = U\tilde{C}U^\dagger$ . The transformation  $U$  being unitary, we have

$$C_{11}(z) = \sum_j |U_{1j}|^2 \tilde{C}_{jj}(z), \quad (23)$$

where the vector of coefficients

$$\left(|U_{1j}|^2\right)_j = (0, 1/4, 1/4, 0, 1/8, 1/8, 1/8, 1/8) \quad (24)$$

satisfies the condition  $\sum_j |U_{1j}|^2 = 1$ .

The damping rates  $\tilde{\Gamma}_{jj}$  are calculated to second-order in terms of the impurity-phonon coupling potential (8). Each rate is given as the convolution of an uncoupled correlation spectrum  $C_{ii}^0(\omega)$  and the dissipation spectrum (47). The derivation is straightforward; we merely give the result

$$\tilde{\Gamma} = \text{diag}(\Gamma_1, \Gamma_1, \Gamma_2, \Gamma_2, \Gamma_3, \Gamma_4, \Gamma_3, \Gamma_4), \quad (25)$$

with

$$\begin{aligned} \Gamma_1 &= \Gamma_0(1 + n(2\Delta)) \\ \Gamma_2 &= \Gamma_0 n(2\Delta) \\ \Gamma_3 &= \Gamma_0(1 + 4n(2\Delta)) \\ \Gamma_4 &= \Gamma_0(3 + 4n(2\Delta)). \end{aligned} \quad (26)$$

Here we have used the Bose occupation factor

$$n(2\Delta) = \frac{1}{e^{\beta 2\Delta} - 1} \quad (27)$$

and the coupled phonon Green function (47) evaluated at the frequency  $2\Delta/\hbar$ ,

$$\Gamma_0 = 2\Gamma''(2\Delta/\hbar) = \pi \sum_{\alpha} f_{\alpha} \frac{\gamma_{\alpha}^2}{v_{\alpha}^5} \frac{(2\Delta)^3}{2\pi^2 \rho \hbar^4}. \quad (28)$$

The geometric factor  $f_{\alpha}$  arises from the different weight for longitudinal and transverse modes in the coupling matrix elements.

Now we have an explicit expression for the frequency dependent function (23). After inverse Laplace transformation we obtain the time-dependent correlation function of the operator  $A_{zz0}$ ,

$$C_{11}(t) = \frac{1}{4} \left( m_1 e^{-\Gamma_1 t} + m_2 e^{-\Gamma_2 t} + m_3 \cos(2\Delta t + \delta_3) e^{-\Gamma_3 t} + m_4 \cos(2\Delta t + \delta_4) e^{-\Gamma_4 t} \right), \quad (29)$$

which constitutes the basic theoretical result of this paper.

As the most salient features we note the presence of two relaxation features with different relaxation rates  $\Gamma_1$  and  $\Gamma_2$ . The remaining terms (the so-called resonant terms) show oscillations with twice the tunneling frequency  $\Delta/\hbar$  and different damping rates, with  $\tan \delta_i = \hbar \Gamma_i / 2\Delta$ . The amplitudes  $m_i$  vary significantly with temperature; in the high-temperature limit all of them tend towards unity,  $m_i \rightarrow 1$ , whereas for  $T \rightarrow 0$  one finds  $m_3 = 4$  and  $m_1 = m_2 = m_4 = 0$ . Thus the relaxation contributions disappear at zero temperature.

The spectra of the response function (12) and the correlation function (29) are related through the fluctuation-dissipation theorem,

$$\chi''(\omega) = (2/\hbar) \tanh(\beta \hbar \omega / 2) C_{11}''(\omega). \quad (30)$$

With the usual approximations for the hyperbolic tangent function we thus obtain

$$\chi''(\omega) = \beta \hbar \omega [L_1(0) + L_2(0)] + \tanh(\beta \Delta) [L_3(2\Delta) - L_3(-2\Delta) + L_4(2\Delta) - L_4(-2\Delta)], \quad (31)$$

with the weighted Lorentzian

$$L_i(E) = \frac{m_i}{4} \frac{\hbar \Gamma_i}{(\hbar \omega - E)^2 + \hbar^2 \Gamma_i^2}. \quad (32)$$

Clearly, the spectrum of the response function  $\chi''(\omega)$  contains the same physics as the correlation function  $C_{11}$ ; hence the discussion below (29) applies equally well to (31).

The tunneling impurities can be probed by an external ultrasonic wave with propagation vector  $\mathbf{k}$  and polarisation vector  $\mathbf{e}^{\alpha}$ . The attenuation of the latter is given by the internal friction

$$Q_{\alpha}^{-1} = n h_{\mathbf{k}\alpha} \frac{\gamma_{\alpha}^2}{\rho v_{\alpha}^2} \chi''(\omega), \quad (33)$$

whereas the variation of the sound velocity

$$\frac{\delta v_{\alpha}}{v_{\alpha}} = n h_{\mathbf{k}\alpha} \frac{\gamma_{\alpha}^2}{2 \rho v_{\alpha}^2} \chi'(\omega), \quad (34)$$



depends on the real part of the impurity dynamic susceptibility  $\chi'$ . Here  $n$  is the number density of the impurities; the geometric factor  $h_{\mathbf{k}\alpha}$ , as defined in (52), accounts for the orientation of  $\mathbf{k}$  and  $\mathbf{e}^\alpha$  with respect to the crystal axes.

Since the tunneling frequency  $\Delta/\hbar$  is of the order of 20 GHz, the second term of (31) is immaterial at acoustic frequencies; and the internal friction involves the relaxational part only,

$$Q_\alpha^{-1} = n h_{\mathbf{k}\alpha} \frac{\gamma_\alpha^2}{\rho v_\alpha^2} \frac{1}{k_B T} \left[ m_1 \frac{\omega \Gamma_1}{\omega^2 + \Gamma_1^2} + m_2 \frac{\omega \Gamma_2}{\omega^2 + \Gamma_2^2} \right]. \quad (35)$$

Note that both amplitudes are exponentially small at low temperatures,  $m_1 + m_2 = 2 * \text{sech}(\beta\Delta/2)^2$ , though  $m_1$  vanishes faster than  $m_2$ . On the other hand,  $\Gamma_1$  tends towards the constant  $\Gamma_0$ , whereas  $\Gamma_2$  disappears. Thus in the intermediate range  $k_B T \approx \Delta$  both contributions may be relevant.

Because of the different temperature dependence of the two rates and the corresponding amplitudes, the variation of  $Q^{-1}$  with frequency changes very much with the ratio  $\omega/\Gamma_0$ . The origin of the terms in (35) is quite obvious in view of the level scheme of Fig. 1. The contribution involving  $\Gamma_2$  stems from relaxation between the states of the level  $T_{1u}$ ; the required intermediate transition to the top level  $A_{2u}$  accounts for the temperature factor of  $\Gamma_2$ . On the other hand, the term with  $\Gamma_1$  results from the upper triple level  $T_{2g}$ ; relaxation occurs through the intermediate state  $A_{1g}$ ; phonon emission in this downscattering process gives rise to the temperature factor of  $\Gamma_1$ . The rates of the resonant contributions in (31) can be discussed in a similar fashion.

Finally we note that the relaxation rates  $\Gamma_1$  and  $\Gamma_2$  satisfy the condition  $\Gamma_1 = e^{\beta 2\Delta} \Gamma_2$ . They are related to the phase decoherence rates  $\Gamma_3$  and  $\Gamma_4$  through  $\Gamma_1 + \Gamma_2 = (1/4)(\Gamma_3 + \Gamma_4)$ ; thus the transverse rates are larger than the longitudinal ones, contrary to the well-known ratio for the two-level system,  $1/T_1 = 2/T_2$ .

### 3.2 Effects of asymmetry

In order to obtain a realistic model for tunnel impurities, we have to account for the random asymmetry fields (10). At sufficiently low concentrations,  $c < 100$  ppm or  $n < 10^{19} \text{ cm}^{-3}$ , typical values of  $v_i$  are significantly smaller than the tunnel energy  $\Delta$ . Thus we may use a perturbation expansion in powers of the small parameter  $v_i/\Delta$ .

Each pole of the dynamic susceptibility (31) is characterized by an amplitude  $m_i$ , a damping rate  $\Gamma_i$ , and an oscillation frequency that takes the values  $\pm 2\Delta$  or 0. It turns out that the lowest-order corrections to  $m_i$  and  $\Gamma_i$  are quadratic in  $v_i/\Delta$  and thus are of little significance. Similarly, the finite poles at  $\pm 2\Delta$  are hardly affected by the small asymmetry energies  $v_i$ .

A significant change occurs, however, in the zero-frequency poles. When evaluating (15) with both (5) and (10) and calculating the lowest-order corrections in the diagonal representation (22), we obtain the set of frequencies

$$\tilde{\Omega} \approx \text{diag}(\eta, \eta, -\eta, -\eta, -2\Delta, -2\Delta, 2\Delta, 2\Delta) \quad (36)$$

with

$$\eta = 1/2 (v_1^2 - v_2^2)/\Delta. \quad (37)$$

Accordingly, the relaxation contributions  $L_1(0)$  and  $L_2(0)$  in (31) have to be replaced by  $\frac{1}{2}(L_i(\eta) + L_i(-\eta))$ , with  $i = 1, 2$ .

Since experimentally frequencies are much smaller than the tunnel frequency  $\Delta/\hbar$ , the imaginary part of the susceptibility is determined by the low-frequency poles  $\pm\eta$ . When denoting the average with respect to the random fields  $v_i$  by a bar, we have

$$\overline{\chi''(\omega)} = \frac{1}{2}\beta\omega \left( \overline{L_1(\eta)} + \overline{L_1(-\eta)} + \overline{L_2(\eta)} + \overline{L_2(-\eta)} \right). \quad (38)$$

When inserting the inverse Fourier transform of the Lorentzians, the integral over  $v_i$  involves a Gaussian with complex width parameter  $(1/2\sigma^2) \pm it/\hbar\Delta$ . Performing the Gaussian integrals we find

$$\overline{\chi''(\omega)} = \beta \frac{\omega\Delta}{4\sigma^2} \int_0^\infty dt \frac{\cos(\tilde{\omega}t)}{\sqrt{1+t^2}} \left( m_1 e^{-\tilde{\Gamma}_1 t} + m_2 e^{-\tilde{\Gamma}_2 t} \right), \quad (39)$$

with  $\tilde{\omega} = \omega\Delta/\sigma^2$  and  $\tilde{\Gamma} = \Gamma\Delta/\sigma^2$ . We recall that we have used  $k_B T, \Delta \gg \hbar\omega, \hbar\Gamma$ .

Now we turn to the real part that is obtained from (30) through the Kramers-Kronig relation. Proceeding as above we insert the inverse Fourier transform; resorting to the usual approximations for the temperature-dependent factors and assuming  $\beta\eta/2 \ll 1$ , we obtain the susceptibility

$$\chi'(\omega) = \frac{m_3 + m_4}{4} \frac{1}{\Delta} \tanh(\beta\Delta) + \beta \sum_{i=1,2} \sum_{\pm} \frac{m_i}{4} \frac{\eta(\eta \pm \omega) + \Gamma_i^2}{(\eta \pm \omega)^2 + \Gamma_i^2}. \quad (40)$$

Averaging over the distribution of asymmetries yields

$$\overline{\chi'(\omega)} \approx \frac{m_3 + m_4}{4} \frac{1}{\Delta} \tanh(\beta\Delta) + \sum_{l=1,2} \frac{m_l}{4} \beta \left\{ 1 - \frac{\omega\Delta}{\sigma^2} \int_0^\infty dt \frac{\sin(\tilde{\omega}t)e^{-\tilde{\Gamma}_l t}}{\sqrt{1+t^2}} \right\} \quad (41)$$

### 3.3 Comparison with a two-level tunneling system

When investigating the dynamic properties of substitutional impurities, various authors have used a two-state approximation. For this reason we briefly discuss the response function of a two-level system (TLS) and compare it with the present results for the eight-state system. With the notation introduced in Sect. 2, the Hamiltonian of a symmetric TLS reads as

$$H = \frac{1}{2}\Delta\sigma_x + \sigma_z \sum_{\alpha,i,j} \gamma_\alpha \epsilon_{ij}^\alpha + H_{\text{phonon}}, \quad (42)$$

which is nothing but the one-dimensional version of (5) and (8). When evaluating the dissipative two-state dynamics one finds that there is no relaxation contribution to the response function of a TLS; its susceptibility is of purely "resonant" character and similar to the second term of (31).

Thus the two-state approximation misses the observed relaxation peak in the dynamic response. In order to mend this failure, an asymmetry energy has been added to (42), yielding

$H = \frac{1}{2}\Delta\sigma_x + \frac{1}{2}\epsilon\sigma_z$ , with a two-level splitting  $E = \sqrt{\Delta^2 + \epsilon^2}$ . The spectrum of the dynamic susceptibility then reads as

$$\chi''_{zz} = \frac{\Delta^2}{E^2} \tanh(\beta E/2) \sum_{\pm} \frac{\pm\Gamma}{(\omega \mp E/\hbar)^2 + \Gamma^2} + \frac{\epsilon^2}{E^2} \text{sech}^2(\beta E/2) \frac{\beta\hbar\omega \cdot (2\Gamma)}{\omega^2 + (2\Gamma)^2}. \quad (43)$$

The amplitude of the relaxation feature is proportional to  $\epsilon^2/E^2$  and thus vanishes in the limit of zero asymmetry energy. This feature distinguishes the actual eight-state system from the two-state approximation. The former contains a strong relaxation feature, even at zero asymmetry energy. The two-state approximation, however, fails to account for relaxation in the symmetric case  $\epsilon = 0$ .

## 4 Experimental detail and results

The crystals measured here were seed pulled from the melt at the crystal growth facility of the Cornell Center for Materials Research. The starting powder of KCl was Merck Industries "Superpure" grade with nominal impurity levels of less than 1 ppm. (A check of the OH<sup>-</sup> level in our crystal of "pure" KCl, via UV absorption, confirmed a concentration of 0.5 ppm.) The cyanide added to the melt was taken from a seed-pulled single crystal of KCN for which the starting powder had been vacuum baked to remove H<sub>2</sub>O.

The composition of the final crystal was analyzed via infra-red absorption ( $\sim 2100 \text{ cm}^{-1}$ ) to an estimated accuracy of 10% relative error, by comparing the area of the absorbance peak to a standard measured for us by Fritz Lüty at the University of Utah where he measured the CN<sup>-</sup> vibrational spectra at liquid nitrogen temperature and calculated the concentration based on the known oscillator strength of CN<sup>-</sup> [13].

The internal friction sample was cleaved directly from the IR absorption sample to ensure a known CN<sup>-</sup> concentration. The internal friction was measured with a composite torsional oscillator as described in Ref. [14]. In this method, a 90 kHz quartz transducer (2.5 mm diameter) and the sample form a composite torsion bar. The quartz end is attached to a thin Be-Cu pedestal [14] by an approximately 25 mg drop of Stycast 2850FT epoxy, and since the KCl crystals are quite fragile, a 0.25 mm indium foil was epoxied between the crystal and transducer to "cushion" the difference in thermal contraction rates of the two components upon being cooled. The sample length is tuned to be one half of a shear wavelength, so that the composite oscillator has a resonance frequency at room temperature within 1% of the bare quartz crystal resonance. This adjustment ensures that the epoxy and indium joint between the quartz and sample has almost zero strain, and therefore contributes minimally to the observed internal friction. (The epoxy and epoxy/indium junctions produce a background contribution to the internal friction of less than  $10^{-5}$  at low temperatures.)

The oscillator is driven by a set of electrodes which form a quadrupole configuration around the transducer and which simultaneously drive and detect its motion. The internal friction of the sample  $Q_{sa}^{-1}$  is determined from the quality factor  $Q_{comp}$  of the composite oscillator resonance by

$$Q_{sa}^{-1} = \left[ \frac{I_{sa} + (1 + \alpha)I_{tr}}{I_{sa}} \right] Q_{comp}^{-1} \quad (44)$$

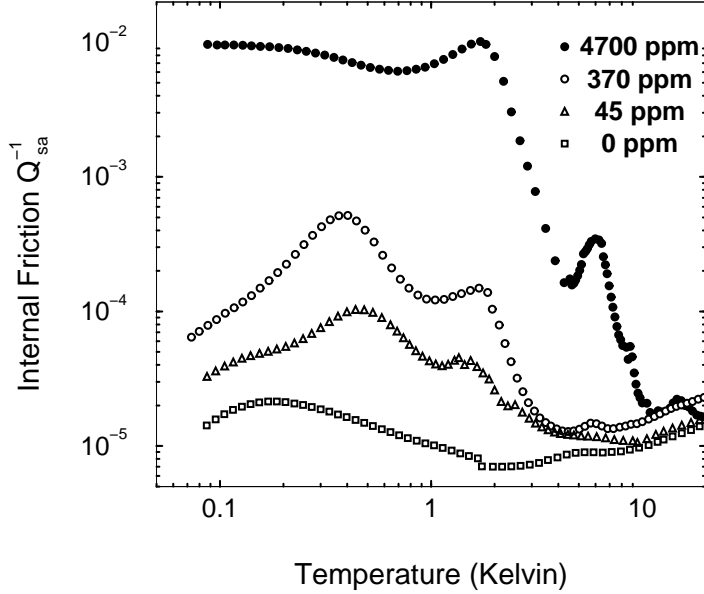


Figure 2: The internal friction data of four KCl samples with different concentrations of  $\text{CN}^-$  dopants are plotted versus the temperature.

where  $I_{tr}$  and  $I_{sa}$  are the moments-of-inertia of the transducer and sample respectively, and  $\alpha$  is a correction for the attachment of the transducer to the thin Be-Cu pedestal,  $\alpha \approx 0.06$ [14]. The relative change in speed of sound can be found from the change in resonance frequency of the composite oscillator

$$\frac{\Delta v}{v_{sa}} = \left[ \frac{I_{sa} + (1 + \alpha)I_{tr}}{I_{sa}} \right] \frac{\Delta f}{f}, \quad (45)$$

where  $\Delta f/f$  is determined relative to an arbitrary reference frequency usually at the coldest temperature of the run. Details on evaluating internal friction from a torsional oscillator can be found in Ref. [15]. The measurements below 1.5 K were made in a dilution refrigerator, and those from 1.5 to 300 K in an insertable  $^4\text{He}$  cryostat [16].

We have investigated a  $T_{2g}$ -mode ( $\hat{\mathbf{e}} = [110]$ ,  $\hat{\mathbf{k}} = [001]$ ) in three samples doped with 45, 370 and 4700 ppm  $\text{CN}^-$ , and a pure sample; the latter provides the background due to the host crystal and thus permits us to determine the impurity contribution to the elastic response function.

Figure 2 shows the internal friction as a function of temperature, cyanide concentration ranging from 0 to 4700 ppm. The data consist of several peaks. The dominant feature occurs at about 450 mK in the 45ppm-data and moves to about 350 mK in the 370ppm-data; in the strongly doped sample (4700ppm) it results in a broad shoulder beyond the lowest temperatures investigated. At higher  $T$  there are additional peaks with much weaker intensity, which may well result from strongly coupled defect pairs [18]. The internal friction of the undoped sample is significantly smaller, although still remarkably high. (Even after a check for purity, there is still some unexpected damping in the “pure” KCl. The expected background internal friction value for pure crystals using this technique is less than  $3 \times 10^{-6}$  below 1 K, as measured in quartz [15].)

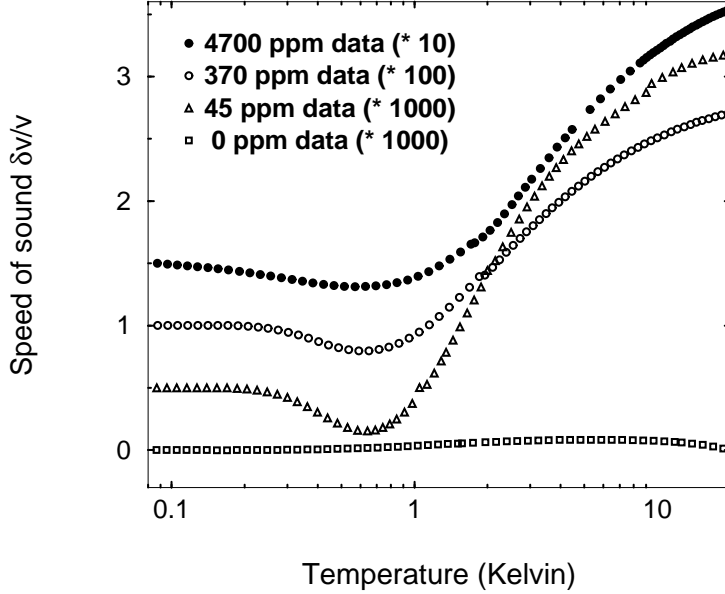


Figure 3: Relative change of sound velocity  $\delta v/v$  for four KCl samples with different concentrations of  $\text{CN}^-$  dopants are plotted versus the temperature. For convenience, the data are multiplied by the factors of 10. Note the vertical shift by steps of 0.5 with respect to the somewhat arbitrary origin at zero temperature.

The relative change of the sound velocity is plotted in figure 3. The temperature dependence of the data may be decomposed in two features. First, there is a contribution proportional to  $\tanh(E/2kT)$  with an energy  $E$  of a few K, that is characteristic for quantum defects and shows the well-known  $1/T$ -dependence at higher temperature. Second, the minimum at  $T = 0.7$  K indicates a relaxation process.

Though the minimum broadens with increasing doping, the three samples show quite a similar behavior, and the change in sound velocity is roughly linear in the impurity concentration.

## 5 Comparison of theory and experiment

We focus on the data of KCL with 45 ppm  $\text{CN}^-$  since our theory is correct for low doping only, i.e. for impurities without interaction. With increasing doping, however, their dipolar interactions are no longer small. The collective dynamics results in the broad internal friction spectrum shown in figure 2 at higher concentrations; the sharp features indicate strongly coupled impurity pairs.

The theoretical expressions for symmetric tunnel impurities involve the tunnel energy  $\Delta$  and the damping rate  $\Gamma_0$  (28); taking also finite asymmetry energies as in Sect. 2.3 into account, the Gaussian width  $\sigma$  provides one more parameter. Both the rate  $\Gamma_0$  and the prefactors of the internal friction and the change of sound velocity (33,34) depend on the deformation potentials  $\gamma_\alpha$ , the sound velocities  $v_\alpha$ , and the mass density of the host crystal  $\varrho$ . The latter quantities are well known; since the longitudinal sound velocity is significantly larger

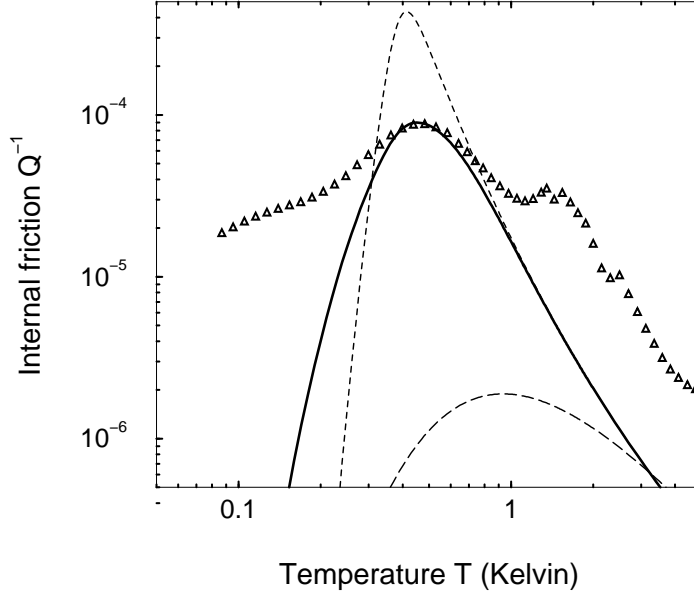


Figure 4: The [111]-defect theory is fitted at the data of the internal friction of the KCl: 45ppm  $\text{CN}^-$  sample. The full line is a fit including asymmetry effects and the short-dashed line without these. The long-dashed line shows a plot of the internal friction of a two-level-system where we set  $(\epsilon/E) = 1$  whereas all other parameters was chosen the same as in the former fit.

than the transverse one, we have  $v_t^{-5} \gg v_l^{-5}$  and retain transverse sound waves only, with  $v_t = 1.7 \text{ km/s}$  and  $\rho = 1.989 \text{ g/cm}^3$ . (We neglect the weak dependence of the sound velocity on the propagation direction.)

The tunnel energy  $\Delta/k_B$  of CN in KCl has been measured by various techniques, with different experimental results; paraelectric resonance: 1.87 K [22]; excitation of optical vibrations: 1.73 K [23]; specific heat: 1.6 K [24]. The relatively large discrepancy between these values may be due to experimental uncertainties and different parameters of the samples, in particular impurity concentration. From our fits to the 45 ppm data we obtained a value of 1.55 K, which is in reasonable agreement with the above results. Regarding the asymmetry energy, we use  $\sigma/k_B = 0.0145 \text{ K}$  for the width of the Gaussian distribution. Finally, the transverse deformation potential  $\gamma_t$  constitutes the most important parameter, appearing both in the prefactors and relaxation rates. From our fits we obtain the value  $\gamma_t = 0.192 \text{ eV}$  which is of the same order of magnitude as the values obtained for OH impurities in KCl (1 eV) [25], in NaCl (1.0 eV) [26] and OD in NaCl (0.34 eV) [26].

First we discuss the internal friction as shown in figure 4. The triangles are the background corrected data of the 45 ppm sample, i.e., we have subtracted from the original data the values for the undoped sample. The full line is a fit including asymmetry effects (39) where we used the parameters given in Table 1.

The temperature where the maximum occurs depends strongly on the tunneling amplitude  $\Delta$  and the fraction  $\omega/\Gamma_0$ ; the maximum value of  $Q^{-1}$  varies with the prefactor and the asymmetry width as far as the mean splitting is bigger than the frequency  $\bar{\eta} = \sigma^2/\Delta \geq \omega$ .

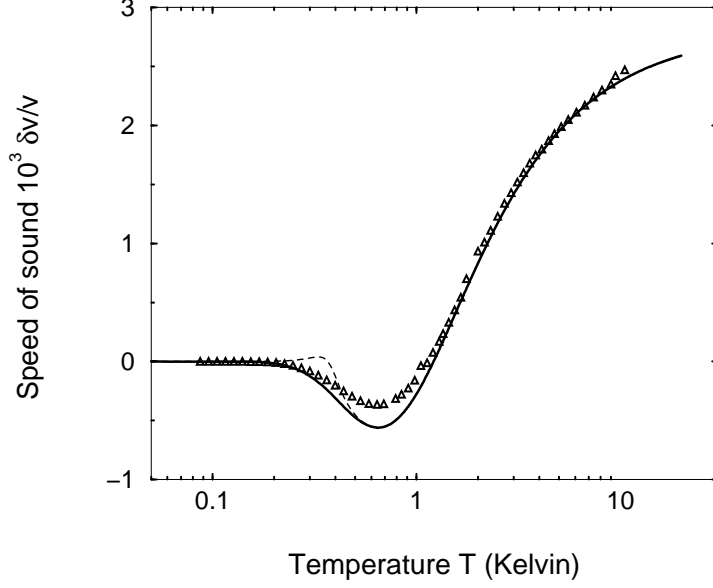


Figure 5: The [111]-defect theory is fitted at the data of the relative change in speed of sound of the KCl: 45ppm  $\text{CN}^-$  sample. The full line is a fit including asymmetry effects and the dashed line without these.

The relaxation peak arises where the external frequency is comparable to the slow rate  $\Gamma_2$ , and  $T_{max}$  is determined by the relation  $\Gamma_2(T_{max}) = \omega$ . Thus the exponential decrease of  $\Gamma_2$  is essential for the existence of the relaxation maximum.

Note that this mechanism does not exist for two-level tunneling systems, even with large asymmetries, since their relaxation rate tends towards a constant  $\Gamma_0$ . As a consequence, for  $\omega \ll \Gamma_0$  the relaxation maximum is suppressed by a factor  $\omega/\Gamma_0$ , and the internal friction of a two-level system is by two orders of magnitude smaller than that obtained for the [111]-impurity model. Note that the parameters gathered in Table 1 result in a rate constant  $\Gamma_0 = 1.35 \times 10^9 \text{ sec}^{-1}$  which is indeed much larger than the frequency  $\omega = 5.3 \times 10^5 \text{ sec}^{-1}$ . For systems with  $\eta > \omega$  the peak is suppressed by  $\omega/\eta$  (see eq.(38)) which means that the peak contribution stems from systems with small asymmetries. Therefore the peak in the internal friction data determines only a combination of the prefactor and the asymmetry width.

Our simple model accounts well for position and height of the peak and for its shape close to the maximum. Yet it strongly underestimates the wings at temperatures well above and below  $T_{max}$ . As to the excess spectral weight observed at low temperatures, a more realistic distribution of asymmetry energies would probably give a better agreement than the Gaussian used in (39). The additional peak at about 2 K may well be due to strongly coupled pairs.

Now we turn to the relative change of sound velocity as shown in figure 5. The triangles are data for the 45 ppm sample. The dashed line is a fit without asymmetry, given by (34), and the full line with asymmetry (41). The asymmetry distribution with width  $\sigma$  merely smears out the temperature dependence. Thus the fit of Fig. 5 mainly depends on the tunneling amplitude and the prefactor but it hardly varies with the relaxation rate and the asymmetry

$\omega/2\pi$ (sec <sup>-1</sup> )	$n$ (cm <sup>-3</sup> )	$\varrho$ (gcm <sup>-3</sup> )	$v_t$ (km/s)	$\Delta/k_B$ (K)	$\gamma_t$ (eV)	$\sigma/k_B$ (K)
84352	$1.7 \times 10^{17}$	1.989	1.7	1.55	0.192	0.0145

Table 1: Parameters used for the fits of Figs. 4 and 5

width.

Regarding both Figs. 4 and 5, our model fits remarkably well the absolute values of  $\delta v/v$  and  $Q^{-1}$ , the hump in the sound velocity, and the position of the relaxation peak in the internal friction. The transverse deformation potential is the most relevant parameter that determines both the absolute values of  $\delta v/v$  and  $Q^{-1}$ , and the relaxation maximum of the latter; we find the value  $\gamma_t = 0.192$  eV. (Note the factor 2 in our definition of the phonon coupling (8).)

The width of the relaxation peak of  $Q^{-1}$  and the low-temperature wing indicate the relevance of the asymmetry energies (10). The poor quality of our fit at low  $T$  may well be due to the choice of a Gaussian distribution for the asymmetries. Nonetheless, our results confirm that for the 45 ppm sample, the mean asymmetry is by two orders of magnitude smaller than the tunnel energy, which is consistent with the model assumptions.

The present theory accounts fairly well for available data on the relaxation behavior of [111]-impurities in alkali halides investigated with  $T_{2g}$ -modes, in particular with respect to the temperature dependence. Yet the multiexponential decay with the two rates  $\Gamma_1$  and  $\Gamma_2$  gives rise to quite an intricate relaxation spectrum; thus an experimental investigation of the frequency dependence would seem most promising. A similar behaviour was also found for an  $E_g$ -mode [9] contradicting the simplest model of an [111]-defect. Even asymmetries can not explain this feature in a simple way. Another open question concerns the thermal conductivity [2]. The relaxation feature obtained in the present work should significantly contribute to thermal resistivity at low  $T$ . Still, the spectrum of the defects obtained from the data [2] suggests a more complicated elastic response spectrum and may well require large asymmetry energies.

Another interesting point would be to extend the present work to the case of strong doping; this is certainly not an easy task, given the serious difficulties encountered already in the treatment of interacting two-state systems (see, e.g., Ref. [27].) Note, however, that our sound velocity data in Fig. 3 depend, roughly speaking, linearly on the impurity concentration. Thus it would seem that they do not fulfil the strong-coupling criterion of [8], i.e., the dipolar interactions have not yet destroyed the coherent tunnel motion.

## 6 Summary

We have investigated the relaxation of an impurity ion in alkali halides arising from the coupling to elastic waves. We briefly summarize the main results.

(i) The various elastic and inelastic phonon-mediated transition between the eight quantum states give rise to an intricate temperature and frequency dependence of the relaxation contributions to the internal friction and the sound velocity (see Fig. 1.) Unlike two-state



tunneling systems, [111]-impurities show two relaxation rates. At low  $T$ , the smaller rate decreases exponentially,  $\Gamma_2 = e^{-2\Delta/kT}\Gamma_0$ , whereas the larger one tends towards a constant,  $\Gamma_1 = \Gamma_0$ . This corresponds to a multiexponential decay of the time-dependent response and correlation functions (12) and (29).

(ii) A most particular relaxation behavior arises for external frequencies  $\omega$  that are smaller than the constant rate,  $\omega < \Gamma_0$ . Then the relaxation maximum occurs at a temperature where the smaller rate  $\Gamma_2$  is equal to the external frequency  $\omega$ . This maximum is the more relevant as at low  $T$  the spectral weight of the slow contribution exceeds by far that of the faster rate  $\Gamma_1$ .

(iii) Comparison with recent data on KCl:CN proves the relevance of this relaxation mechanism. The exponentially decreasing rate  $\Gamma_2$  explains the large amplitude of the relaxation peak shown by the external friction  $Q^{-1}$  as a function of temperature at  $\nu = 84$  kHz. By the same token, our model provides a good description for the hump in the sound velocity.

(iv) The prefactors of  $\delta v/v$  and  $Q^{-1}$  and the relaxation rates are related by the values for the deformation potential  $\gamma$ , sound velocity  $v$ , and mass density  $\rho$ . By taking  $\gamma$  as a free parameter, we obtain for reasonable values of  $\gamma$  (compared with similar materials) satisfying fits for  $\delta v/v$  and  $Q^{-1}$ , involving both absolute values and the temperature dependencies.

(v) The phenomena mentioned in (iii) cannot be explained in terms of relaxation of corresponding two-level systems. For the latter, the low-temperature rate tends towards a constant and thus may exceed  $\omega$  at any  $T$ , whereas the small rate  $\Gamma_2$  of a [111]-impurity inevitably meets  $\omega$  at some  $T$  and gives rise to a relaxation peak. Though certain aspects of the thermal and dielectric properties of such doped crystals are described by an ensemble of two-state systems, such a model fails in view of the acoustic properties, due to the multiexponential decay of the elastic response function (12).

**ACKNOWLEDGEMENTS** We would like to express a special thank you to Prof. Robert Pohl for his guidance on the experiments as well as many stimulating discussions and helpful comments on this manuscript. We also wish to thank C. Enss for stimulating the theoretical investigation and H. Horner, R. Kühn and B. Thimmel for many helpful discussions. Additionally P. Nalbach wants to thank the DFG which supported the work within the DFG-project HO 766/5-3 "Wechselwirkende Tunnelsysteme in Gläsern und Kristallen bei tiefen Temperaturen".

## A Geometric factor of the ESS

Time evolution of the phonon heat bath is given by the lattice response function ( $t \geq 0$ )

$$\Gamma(t) = \sum_{\alpha} \frac{\gamma_{\alpha}^2}{\hbar^2} \overline{\langle [\epsilon_{ij}^{\alpha}(t), \epsilon_{ij}^{\alpha}] \rangle}, \quad (46)$$

where  $i \neq j$  and the bar indicates the average over crystal axes. The entries of the damping matrix (18) are determined by the coupled phonon spectrum; in the limit of long wavelengths one has

$$\Gamma''(\omega) = \frac{\pi}{2} \sum_{\mathbf{k}\alpha} f_{\mathbf{k}\alpha}^{(ij)} \gamma_{\alpha}^2 \frac{k^2}{m\hbar\omega_{\mathbf{k}\alpha}} [\delta(\omega - \omega_{\mathbf{k}\alpha}) - \delta(\omega + \omega_{\mathbf{k}\alpha})], \quad (47)$$

where

$$f_{\mathbf{k}\alpha}^{(ij)} = \left( e_i^\alpha(\mathbf{k}) \hat{k}_j + e_j^\alpha(\mathbf{k}) \hat{k}_i \right)^2 \quad (48)$$

accounts for the orientations of wave and polarizations vectors with respect to the crystal axes. For an isotropic phonon density of states, the sum over phonon modes becomes

$$\frac{1}{V} \sum_{\mathbf{k}, \alpha} f_{\mathbf{k}\alpha}^{(ij)}(\dots) \longrightarrow \frac{1}{2\pi^2} \sum_{\alpha} f_{\alpha} \int_0^K dk k^2(\dots) \quad (49)$$

where we have for each polarization defined the average value

$$f_{\alpha} = \frac{1}{4\pi} \int d\Omega f_{\mathbf{k}\alpha}^{(ij)}. \quad (50)$$

In the Debye model with  $\omega_{\mathbf{k}\alpha} = v_{\alpha} k$ , the damping spectrum finally reads as

$$\Gamma''(\omega) = \frac{\pi}{2} \sum_{\mathbf{k}\alpha} f_{\alpha} \frac{\gamma_{\alpha}^2}{v_{\alpha}^5} \frac{\omega^3}{2\pi^2 \rho \hbar}. \quad (51)$$

Since an elastic wave couples via each of the quadrupole operators to the defect according to (8), the geometric factor  $h_{\mathbf{k}\alpha}$  of the internal friction and the relative change of the sound velocity of an elastic wave with propagation vector  $\mathbf{k}$  and polarisation vector  $\mathbf{e}^\alpha$  gets

$$h_{\mathbf{k}\alpha} = f_{\mathbf{k}\alpha}^{(12)} + f_{\mathbf{k}\alpha}^{(13)} + f_{\mathbf{k}\alpha}^{(23)} \quad (52)$$

The factors  $f_{\alpha}$  are easily evaluated after expressing the unit vectors  $\hat{\mathbf{k}} = \mathbf{k}/k$  and  $\mathbf{e}$  in polar coordinates  $\theta$  and  $\phi$ . Putting  $\hat{\mathbf{k}} = (\sin \theta \sin \phi, \sin \theta \cos \phi, \cos \theta)$ , one finds for the longitudinal case  $\mathbf{e}^1 = \hat{\mathbf{k}}$  the factor  $f_l = 4/15$ .

Regarding the transverse modes, we obtain  $f_{t_2} = 8/45$  for  $\mathbf{e}^2 = (\cos \phi, -\sin \phi, 0)$  and  $f_{t_3} = 2/9$  for the remaining polarization  $\mathbf{e}^3$ . Though these values depend on the choice of  $\mathbf{e}^2$  and  $\mathbf{e}^3$ , their average  $f_t = (1/2)(f_{t_2} + f_{t_3}) = 1/5$  is independent of the basis. Defining moreover the mean value of the three polarisation directions,  $f = (1/3)(f_l + 2f_t)$ , we finally have

$$f_l = \frac{4}{15}, \quad f_t = \frac{1}{5}, \quad f = \frac{2}{9}. \quad (53)$$

Thus the quantity (48) for longitudinal modes is by a factor  $f_l/f_t = 4/3$  larger than for the transverse ones. In the average, propagation and polarisation directions are uncorrelated, resulting in

$$f = \left( \langle \hat{k}_i^2 \rangle \langle e_j^2 \rangle + \langle \hat{k}_j^2 \rangle \langle e_i^2 \rangle \right) = 2(1/3)^2 \quad (54)$$

## References

- [1] M. Gomez, S. P. Bowen, J. A. Krumhansl: Phys. Rev. B **153**, 1009 (1967)
- [2] V. Narayanamurti, R. O. Pohl: Rev. Mod. Phys. **42**, 201 (1970)
- [3] P. Nalbach, O. Terzidis, J. Phys. Condens. Matter **9**, 8561 (1997)

- [4] M.E. Baur, W.R. Salzman: Phys. Rev. **178**, 1440 (1969)
- [5] M.W. Klein: Phys. Rev. B **29**, 5825 (1984); Phys. Rev. B **31**, 2528 (1985)
- [6] T. Kranjc: J. Phys. A **25**, 3065 (1992)
- [7] O. Terzidis, A. Würger: J. Phys. Cond. Matt. **8**, 7303 (1996) ; O. Terzidis: Doktorarbeit, Ruprecht-Karls-Universität Heidelberg 1995
- [8] A. Würger, From coherent tunneling to relaxation, Springer Tracts in Modern Physics Vol. 135, Springer Berlin Heidelberg New York (1997)
- [9] N.E. Byer, H.S. Sack: phys. stat. sol. **30**, 569 (1968)
- [10] M. Hübner, Diplomarbeit, Ruprecht-Karls-Universität Heidelberg 1994
- [11] H. Mori, Prog. Theor. Phys. **33**, 127 (1965); R. Zwanzig, J. Chem. Phys. **33**, 1338 (1960)
- [12] K. A. Topp, PhD-thesis, Cornell University 1997
- [13] F. Lüty, Phys. Rev. B **10**, 3677 (1974).
- [14] David G. Cahill and J.E. Van Cleve, Rev. Sci. Instrum. **60**, 2706 (1989).
- [15] K. A. Topp, E. Thompson, and R.O. Pohl, Phys. Rev. B **60**, 898 (1999).
- [16] E.T. Swartz, Rev. Sci. Instrum. **57**, 2848 (1986).
- [17] J. Classen, C. Enss, C. Bechinger, G. Weiss, S. Hunklinger: Ann. Physik **3**, 315 (1994)
- [18] C. Enss, private communication
- [19] J. Jäckle: Z. Phys. **257**, 212 (1972)
- [20] S. Hunklinger, A.K. Raychaudhuri: Progress in Low-Temperature Physics, ed. by D.F. Brewer, Elsevier Amsterdam (1986)
- [21] A. Würger, in: P. Esquinazi (ed.): Tunneling Systems in Amorphous and Crystalline Solids, Springer Berlin Heidelberg New York (1998)
- [22] F. Holuj, F. Bridges: Phys. Rev. B **20**, 3578 (1979)
- [23] F. Lüty: Phys. Rev. B **10**, 3677 (1974)
- [24] P.P. Peressini, J.P. Harrison, R.O. Pohl: Phys. Rev. **182**, 939 (1969)
- [25] S. Roberts: Phys. Rev. **81**, 865 (1951)
- [26] M. Burst: Diplomarbeit, Universität Karlsruhe 1999
- [27] R. Kühn, A. Würger, Phys. Rev. B (submitted)